INTERNATIONAL JOURNALOF ADVANCED STUDIES
IN COMPUTER SCIENCE AND ENGINEERING 02/28/2021
IJASCSE VOULME 10 ISSUE 2, 2021

Efficient Thermal Tunning of Photonic Devices

Pariwash Iftikhar*
Department of Telecommunication Engineering,
Mehran University of Engineering & Technology
Jamshoro 76062 Sindh Pakistan
*Corresponding author
e-mail: pariiwash@gmail.com

Faisal Ahmed Memon
Department of Telecommunication Engineering,
Mehran University of Engineering & Technology
Jamshoro 76062 Sindh Pakistan
e-mail: faisal.memon@faculty.muet.edu.pk

***Abstract*— In this paper, we exploit high refractive index silicon oxycarbide (SiOC) thin films. SiOC thin films deposited by RF sputtering were used to simulate, design, and fabricate photonic devices such as channel waveguides and Mach-Zehnder interferometers (MZIs). The fabricated micro-photonic structures were tested on a controlled optical setup to estimate the thermo optic coefficient (TOC) at the standard telecommunication wavelength 1550 nm. With refractive index of 2.2 the thermo-optic coefficient of silicon oxycarbide using Mach-Zehnder interferometer was measured as 2.6 x 10^{-4} RIU/℃ that is highest among the dielectric platforms. Our research presents silicon oxycarbide as potential platform for the realization of highly efficient reconfigurable integrated photonic systems.**

Keywords- Integrated photonics; coupler; SiOC; photonics; Mach Zehnder Interferometer.

I. INTRODUCTION

Optical communication has played a vital role in today's era due to its fast speed, reliability and low losses compared to electronic communication platform. These have laid grounds for the emerging science of Integrated Photonics which has enhanced significantly over a few decades. It is realized to be an important technology for future generation's data centers, optical switching and computing, and communication systems due to its compactness, compatibility, and scalability. Few conventional material platforms have been a focus for this field such as, indium phosphide (InP), silicon (Si), silicon dioxide (SiO_2), silicon nitride (SiN) but these material platforms have a constrained refractive index tuning property. The refractive index of a material describes how fast light will travel through that material and is denoted by n. Its formula is n=c/v where c is the speed of light in vacuum and v is the phase velocity of light. The phenomena of the change in refractive index by altering the temperature and at constant pressure is known as thermo optic effect (TOE) and the thermo optic coefficient (TOC) is denoted by dn/dT which is usually used to characterize a material platform. Such material platform like silicon oxynitrate (SiON), a compound of silicon nitride and a dielectric material platform, has been observed to have a flexible tuning of its refractive index that lies between silicon dioxide and silicon carbide [1], [2] where it still shows an absorption peak around 1.5 um wavelength along with the cracks that tend to appear in its geometry when n is greater than 1.5 resulting in higher losses which actually limits its use to low refractive index supporting devices and hence is not suitable to be used for large scale integration. In photonics, for denser integration on a small chip we need a dielectric material with high refractive index or one which supports tunability of its refractive index. One such dielectric material, silicon oxycarbide (SiOC), is suggested in this paper which under varying conditions and a small change in its composition can have a flexible refractive index lying between 1.45 (glass) and 3.2 (silicon carbide) [3], [4]. Generally, Chemical Vapor Deposition (CVD) [5] and sol-gel pyrolysis [6] methods have used to deposit SiOC which contain amounts of hydrogen causing intrinsic losses in material. Whereas, recent studies show that SiOC material waveguides can be deposited using rf sputtering where it responds with low losses [7]. Comprehensive details on structural and chemical properties of SiOC can be found in literature [7]–[9]. As SiOC is found to be a versatile material, it is suggested to have many applications as such Li-ion batteries [10], and interlayer dielectric [11], photoluminescence [12]–[14] and others [15], [16]. Therefore, in this paper, SiOC is used as a dielectric material platform to design such a photonic passive device, a Mach-Zehnder Interferometer (MZI), based on a multimode interference (MMI) coupler as one of its applications. Many devices based on a MMI approach can be present on photonic integrated circuits (PICs) like tunable coupler [17], [18], modulator, optical filter [19]–[24],switch [25], add-drop multiplexer [26], ring lasers [27], and so on.

MZI is one of a complex micro-photonic structure for PICs which can be used as a basic cell to procure the devices stated above. MZI can be constructed using 2 x 2 two 3 dB directional couplers (DCs) or 2 x 2 two 3 dB MMI couplers which can be linked together by a straight and an imbalance waveguide. The power coupled in both the waveguides can be controlled by changing the gap between them or by adjusting the length of directional coupler where as in MMI based MZI it can be controlled by varying the width of the

center multimode section where MMI occur. Practically, it is hard to control the fabrication error that can occur while fabricating a directional coupler as the process require a strict control and DCs are very sensitive towards it. Whereas, most of the devices based on MMI effect have small device dimensions and have better fabrication tolerances.

In this paper, we have analyzed and reported the simulated and experimental results such as effective refractive index and TOC, which is higher by an order of magnitude than that of silicon nitride and 30 x greater than that of silica, of a 2 x 2 SiOC dielectric material based MZI using a directional coupler and using MMI approach. This paper is divided in three sections. After a brief introduction of this paper the section describing the methodology of constructing a MZI is defined. Later, the results obtained by implementing the methodology are discussed and compared. Furthermore, the last section ends with the conclusion defining which of the approach is more feasible to realize a MZI for integration with other photonic devices on a small chip.

II. Simulation Details

A. *MZI with Directional Coupler*

Directional coupler couples the power from one waveguide to the other and vice versa and the coupling ratio depends on the gap between the two waveguides along with the length of the waveguides. It can have various power splitting ratios such as 20%/80%, 90%/10%, 50%/50% (3db coupling) [28]. In photonics, it can be used as a switch or a multiplexer [29]. The DC used in this paper can be explained by Fig. 1.

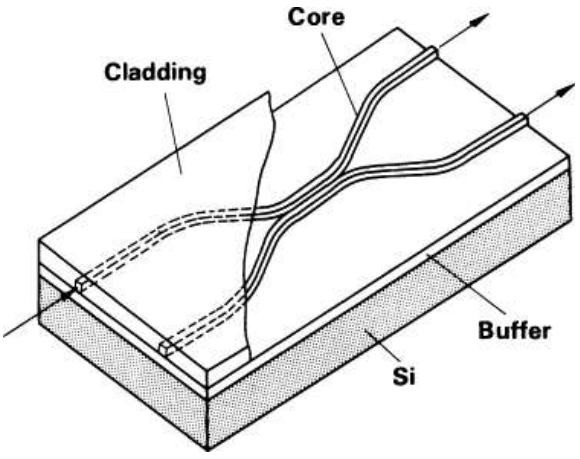

Figure 1. A 3-D Image of a Directional Coupler

The core material of the waveguides of the DC used in this paper is based on SiOC material (n_{core} = 2.2) and the upper and lower cladding are of silicon dioxide ($n_{cladding}$ = 1.45). The coupler consists of two waveguides which are separated in the middle section (length of the coupler) by the coupler gap L_{gap}. The input and output sides have a much larger gap so that the modes traveling in the waveguides do not overlap each other and the coupling can break easily.

A beam propagation method software (BeamPROP) by RSoft was used to simulate and extract the values of effective refractive index (n_{eff}) of the modes propagating in the middle section of a directional coupler. Here, by varying the width and height of the waveguides we obtained optimal values for a single mode operation as multiple modes introduce much complexities. The parameters of waveguides defined for this research were width, height, refractive index of core and cladding, index difference, the designed model's dimensions and many more. Width and height of the waveguides was selected to be 1.3 and 0.175 microns using the refractive index of core and cladding described above hence having the index difference to be 0.75 which is simply the difference of refractive index of core and cladding and index contrast to be 28.28%. The index contrast (Δn) can be found using the formula:

$$\Delta n = (n^2_{core} - n^2_{clad})/2n^2_{core} \quad (1)$$

To find the coupling power in the center section on DC we need the values of n_{eff} for transverse electric TE fundamental even and odd mode at different values of coupler gap. These values were calculated by running the simulations and are presented in which, we can observe that at 0.9 microns of coupler gap n_{eff} even and n_{eff} odd are found to be 1.5607 and 1.5566 respectively. Similarly, with various values of coupler gap with the difference od 1.8 microns we obtained even and odd effective refractive index values of the fundamental mode.

The even n_{eff} is always greater than the value of odd n_{eff} and these values are used to find the propagation constant β value. The field coupling coefficient 'k' depends on the difference between the values of propagation constants of effective indices of the odd and even mode. The propagation constant can be calculated using, $\beta = (2\pi/\lambda)\, n_{eff}$ and the field coupling coefficient is calculated using $k = (\beta_{even} - \beta_{odd})/2$.

B. *MZI with Multimode Interference Approach*

A multimode interference coupler works on self-imaging principle by which the input field is reproduced as mirrored or direct single images, or two-fold images after certain intervals along the direction of length/propagation of the coupler [30]. This principle works in the central multimode waveguided section as there are multiple modes introduced in it. Along with central structure, there are access waveguides to induce and recover light from both of its ends. Generally, these photonic devices are referred as M x

N MMI couplers, where M states the number of input and N states the number of output waveguides. These access waveguides are quite often single-mode waveguides to get a high performance MMI.

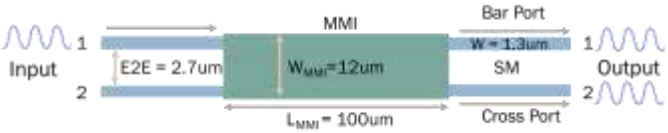

Figure 2. A 2 x 2 MMI Coupler

There are two types of modal excitations in a MMI coupler, one in which no particular modes are excited in the input field (General Interference) and another where certain modes are excited and few modes are blocked using specific excitation inputs (Restricted Interference) [31]. A 3dB coupler based on the latter phenomenon using paired interference pattern is simulated in this paper to construct an MZI.

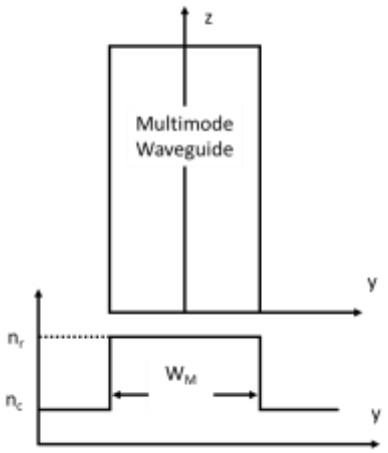

Figure 3. A 2-D image of multimode waveguide with effective index profile and top view

In RSoft's BeamPROP software [32], the SiOC based MMI parameter values defined for a multimode section are set according to the calculated values in which the length of the multimode section can be defined using:

$$L_\pi = (4n_r * W_e^2) / (3\lambda_o) \quad (2)$$

Here, n_r represents the (effective) refractive index of the core material that is based on SiOC and W_e is the effective width corresponding to the fundamental mode, and for high index contrast waveguides, the mode penetration depth is quite small so that it can also be approximated as W_M so that, $W_e \simeq W_M$ which here is 12 um. λ_o here represents the free space wavelength here which is the telecom wavelength 1550 nm. Therefore, the length calculated for 3dB coupling in the multimode section is 100 microns. The field propagation at optimal length is shown in the figures below.

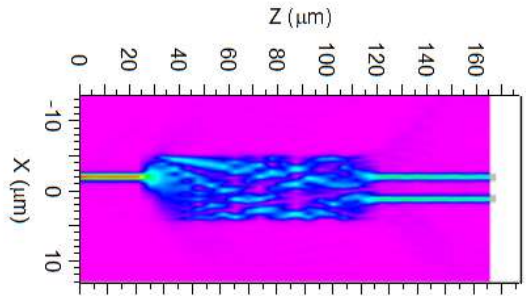

Figure 4. A BeamPROP result showing 3 dB coupling at 100 ums of length of SiOC based MMI

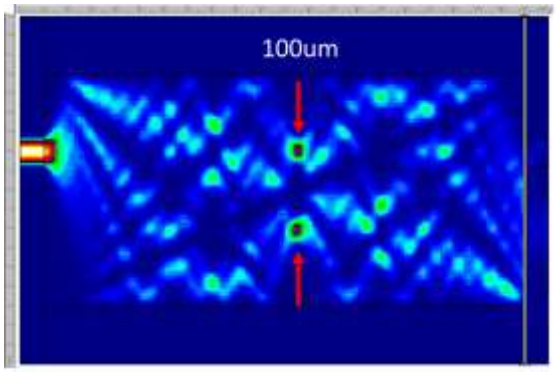

Figure 5. A Fimmwave software image result showing 3 dB coupling at 100 ums of length of SiOC based MMI

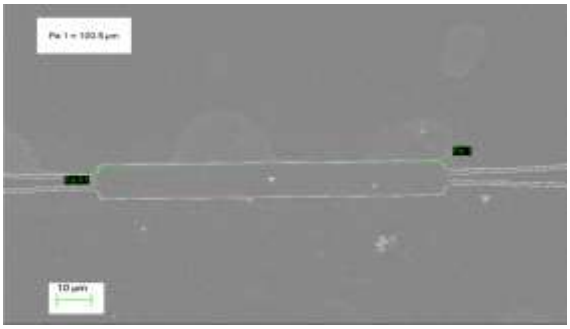

Figure 6. An image of fabricated SiOC based MMI with 100 ums of length

The position of access waveguides to attain the selective excitation of modes is by launching an even symmetric input field at $y = \pm W_e / 6$. In this case, y is ± 2 um. The width of access waveguides is set to be 1.3 um so that the edge to edge gap between two waveguides is 2.7 microns. Bar port refers to a state where output is taken from same

input waveguide and in cross port the output is taken from different waveguide.

III. RESULTS

In DC, coupling power measurements will show us the power transfer from one waveguide to other. Therefore, to calculate the coupling power of a DC we ran few calculations using the formula, $P = \sin(k*L_c)^2$. Here, as defined earlier in text, k is the field coupling coefficient and L_c is the length of coupler under observation.

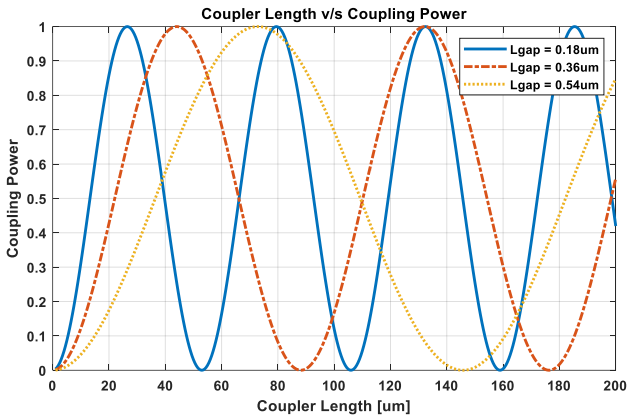

Figure 7. A MATLAB plot showing Coupling Power Ratio between coupling length in microns and coupling power

While increasing the gap between waveguides we can observe that the length of coupling has also increased. Similar results were observed when updating the value of gap between waveguides from 0.18 microns to 1.8 microns.

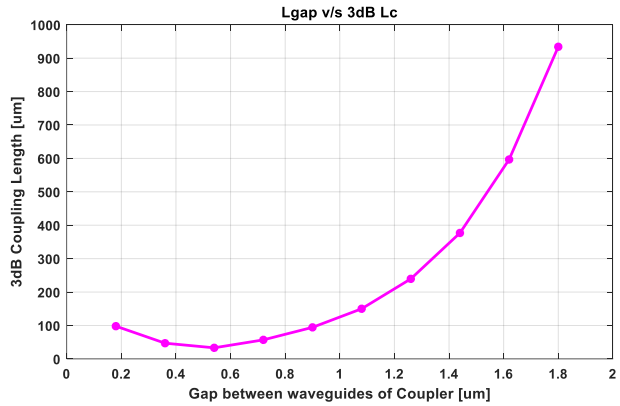

Figure 8. A MATLAB graph showing 3dB coupling at different waveguide gap

Taking the values for 3dB coupling, 50% power transfer, and plotting those against the gap of waveguides of coupler as shown in Fig. 7, we observed that even if the coupling gap between the two waveguides is 1 micron, the length of 3dB coupling section is in between 100 to 150 microns. While at 1.2 L_{gap}, the length of coupling section is approximately 200 microns whereas till 1.8 microns the exponential increase in the 3dB coupling length can be observed. The magnitude of these values of Lc is quite high for fabrication on a small chip which in the end kills the purpose of large-scale integration on a single photonic chip. Another reason for not using DC to create MZI is that the fabricating machine for photolithography, a process to transfer a simulated design or pattern on a polymer substance that is later converted into a hand held photonic chip, is unable to open wide enough to fabricate patterns of less than 2 microns dimensions. Therefore, moving on towards a Mach Zehnder Interferometer based on MMI approach while simulating the design using the above-mentioned parameters, we concluded that the multimode interferometer provides us with 3 dB coupling in a very reasonable length of only 100 ums. Also, the edge to edge gap between two access waveguides is greater than 2 microns i.e, 2.7 microns, which is easy to fabricate and it is not prone to fabrication losses.

The free spectral range (FSR) of a MZI was found to be 4.6 um. The cross talk of experimental results was greater than 30 dB and the extinction ratio was found out to be 10 dB. We can observe while comparing Fig. 9 and Fig. 10 that both results are in agreement which means the simulated results are verified by the experimental results.

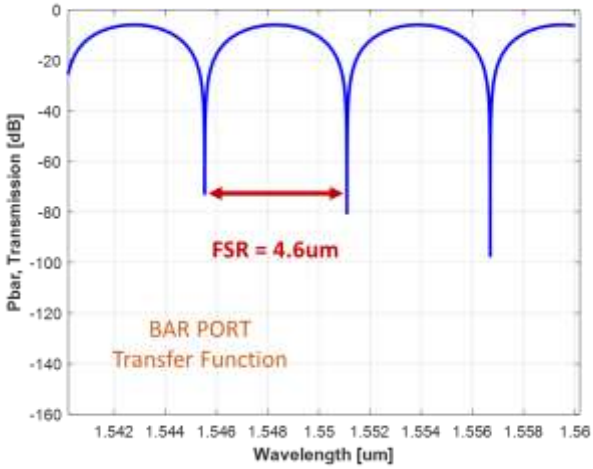

Figure 9. Simulated transfer function (TF) of MZI (Bar Port)

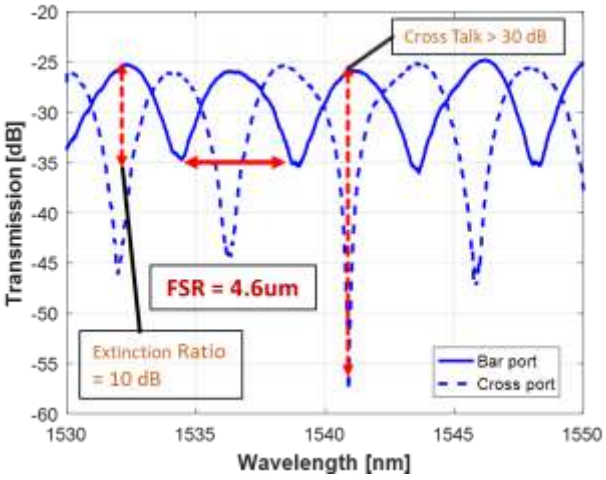

Figure 10. Experimental TF of MZI (Bar and Cross Port)

Now, by varying a degree Celsius temperature of micro fabricated SiOC based MZI we can observe the induced temperature shift of 105 pm per degree Celsius. We can visualize the shift by the change in five degrees per Celsius in the transfer function (TF) of MZI in Fig. 11.

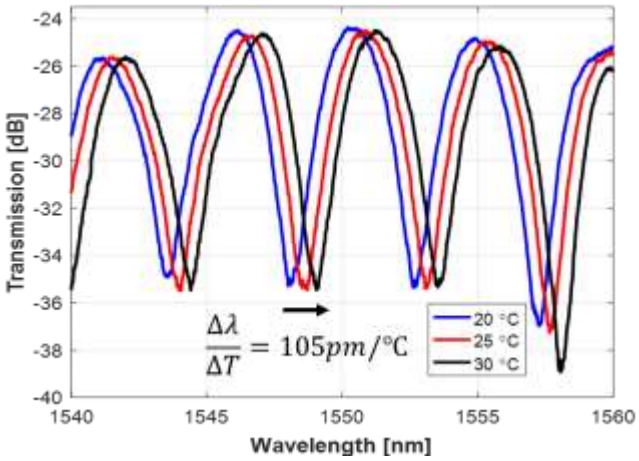

Figure 11. Thermally induced phase shift in TF of SiOC based MZI

$$K_{eff} = (n_g/\lambda) * \Delta\lambda/\Delta T = 1.32 \times 10^{-4}/\,℃ \qquad (4)$$

Here, K_{eff} is the effective TOC of SiOC waveguide [26], n_g is the group index. The TOC of SiOC based MZI K_{SiOC} resulted in 3 x 10^{-4}. This is the largest among all dielectric platforms. We can clearly see the comparative difference between multiple dielectric material platforms in Table 1.

TABLE I. TOC OF VARIOUS DIELECTRIC MATERIALS

Dielectric Materials	Optical Properties of Dielectrics	
	Refractive Index 'n'	*TOC [℃]*
Silica (SiO_2)	1.44 – 1.46	9 x 10^{-6}
Silicon oxynitrate (SiON)	1.45 – 1.46	1.1 x 10^{-5}
Silicon nitride (Si_3N_4)	1.99	2.5 x 10^{-5}
Silicon oxycarbide (SiOC)	1.45 – 3.2	3 x 10^{-4}

IV. CONCLUSION

This paper appraises the use of SiOC, a novel dielectric material, in PICs by the means of micro fabricated photonic devices. A 2 × 2 SiOC based directional coupler was simulated to construct a MZI but due to its photolithography limitations its fabrication had to be halted, thus forcing us to shift our focus to construct the MZI using MMI approach which resulted in its smooth and improved fabrication. The TOC of SiOC based MZI was calculated to be 3 x 10^{-4} which is found to be 30 times higher than that of Silica (SiO_2)[33] and 10 times greater than that of Silicon Nitride (Si_3N_4) [34]proving an efficient platform for large scale integration. Hence, regardless of its high absorption coefficient, making SiOC an improved platform in the field of photonics which can be explored further for future photonic applications.

V. FUTURE WORK

This work provides a futuristic approach in the domain of integrated photonics, where using a high TOC dependent novel material, SiOC, the thermal tuning of photonic waveguides and other passive devices has been made possible which leads to small fabrication sizes along with reduction of large heater sizes and paves a way for further enhancements.

ACKNOWLEDGMENT

Pariwash Iftikhar acknowledges the support received from department of Telecommunication Engineering and IICT directorate at Mehran University of Engineering & Technology, Jamshoro.

REFERENCES

[1] H. Nejadriahi, A. Friedman, R. Sharma, S. Pappert, Y. Fainman, and P. Yu, "Thermo-optic properties of silicon-rich silicon nitride for on-chip applications," *arXiv*, vol. 28, no. 17, pp. 24951–24960, 2020, doi: 10.1364/oe.396969.

[2] A. E. Kaloyeros, Y. Pan, J. Goff, and B. Arkles,

"Review—Silicon Nitride and Silicon Nitride-Rich Thin Film Technologies: State-of-the-Art Processing Technologies, Properties, and Applications," *ECS J. Solid State Sci. Technol.*, vol. 9, no. 6, p. 063006, 2020, doi: 10.1149/2162-8777/aba447.

[3] F. A. Memon *et al.*, "Synthesis, Characterization and Optical Constants of Silicon Oxycarbide," *EPJ Web Conf.*, vol. 139, pp. 0–4, 2017, doi: 10.1051/epjconf/201713900002.

[4] F. A. Memon, F. Morichetti, and A. Melloni, "Waveguiding light into silicon oxycarbide," *Appl. Sci.*, vol. 7, no. 6, pp. 1–11, 2017, doi: 10.3390/app7060561.

[5] S. Gallis, V. Nikas, E. Eisenbraun, M. Huang, and A. E. Kaloyeros, "On the effects of thermal treatment on the composition, structure, morphology, and optical properties of hydrogenated amorphous silicon-oxycarbide," *J. Mater. Res.*, vol. 24, no. 8, pp. 2561–2573, 2009, doi: 10.1557/jmr.2009.0308.

[6] C. Liu *et al.*, "High temperature structure evolution of macroporous SiOC ceramics prepared by a sol–gel method," *Ceram. Int.*, vol. 41, no. 9, pp. 11091–11096, Nov. 2015, doi: 10.1016/j.ceramint.2015.05.056.

[7] F. A. Memon, F. Morichetti, and A. Melloni, "Exploring silicon oxycarbide films for photonic waveguides," *Proc. 2018 15th Int. Bhurban Conf. Appl. Sci. Technol. IBCAST 2018*, vol. 2018-Janua, no. 1, pp. 43–44, 2018, doi: 10.1109/IBCAST.2018.8312182.

[8] C. G. Pantano, A. K. Singh, and H. Zhang, "Silicon oxycarbide glasses," *J. Sol-Gel Sci. Technol.*, vol. 14, no. 1, pp. 7–25, 1999, doi: 10.1023/A:1008765829012.

[9] R. H. Doremus and S. Prochazka, "Silicon oxycarbide glasses: Part II. Structure and properties," *J. Mater. Res.*, vol. 6, no. 12, pp. 2723–2734, 1991, doi: 10.1557/JMR.1991.2723.

[10] L. David, R. Bhandavat, U. Barrera, and G. Singh, "Silicon oxycarbide glass-graphene composite paper electrode for long-cycle lithium-ion batteries," *Nat. Commun.*, vol. 7, 2016, doi: 10.1038/ncomms10998.

[11] X. Huang *et al.*, "Cowpea-like N-Doped Silicon Oxycarbide/Carbon Nanofibers as Anodes for High-Performance Lithium-Ion Batteries," *ACS Appl. Energy Mater.*, vol. 4, no. 2, pp. 1677–1686, Feb. 2021, doi: 10.1021/acsaem.0c02834.

[12] M. Jain, J. R. Ramos-Serrano, A. Dutt, and Y. Matsumoto, "Photoluminescence properties of thin-film SiOxCydeposited by O-Cat CVD technique using MMS and TEOS," *2020 17th Int. Conf. Electr. Eng. Comput. Sci. Autom. Control. CCE 2020*, pp. 5–10, 2020, doi: 10.1109/CCE50788.2020.9299113.

[13] M. Jain, J. R. Ramos-serrano, A. Dutt, and Y. Matsumoto, "The influence of deposition time on the photoluminescent properties of SiO x C y thin films obtained by Cat-CVD from monomethyl silane precursor," *Mater. Lett.*, vol. 291, p. 129547, 2021, doi: 10.1016/j.matlet.2021.129547.

[14] B. Ford, N. Tabassum, V. Nikas, and S. Gallis, "Strong photoluminescence enhancement of silicon oxycarbide through defect engineering," *Materials (Basel).*, vol. 10, no. 4, 2017, doi: 10.3390/ma10040446.

[15] Z. Lin *et al.*, "Strong blue light emission from Eu-doped SiOC prepared by magnetron sputtering," *Int. Symp. Photonics Optoelectron. 2015*, vol. 9656, p. 96560R, 2015, doi: 10.1117/12.2197518.

[16] S. Prucnal, J. M. Sun, W. Skorupa, and M. Helm, "Switchable two-color electroluminescence based on a Si metal-oxide- semiconductor structure doped with Eu," *Appl. Phys. Lett.*, vol. 90, no. 18, 2007, doi: 10.1063/1.2735285.

[17] K. Ogusu, "All-optical switching in nonlinear multimode interference couplers," *Jpn. J. Appl. Phys.*, vol. 51, no. 8 PART 1, 2012, doi: 10.1143/JJAP.51.082503.

[18] Z. Lu *et al.*, "Broadband silicon photonic directional coupler using asymmetric-waveguide based phase control," *Opt. Express*, vol. 23, no. 3, p. 3795, 2015, doi: 10.1364/oe.23.003795.

[19] P. Rabiei, W. H. Steier, C. Zhang, and L. R. Dalton, "Polymer micro-ring filters and modulators," *J. Light. Technol.*, vol. 20, no. 11, pp. 1968–1975, 2002, doi: 10.1109/JLT.2002.803058.

[20] S. Pal and S. Gupta, "Analysis of silicon racetrack modulator employing coupling modulation via active MMI coupler," *IEEE Trans. Nanotechnol.*, vol. 18, no. Il, pp. 392–400, 2019, doi: 10.1109/TNANO.2019.2909147.

[21] H. Abdul Razak, H. Haroon, and A. S. Mohd Zain, "Performance analysis of MMI couplers for modulators on SOI," *ARPN J. Eng. Appl. Sci.*, vol. 11, no. 10, pp. 6275–6278, 2016.

[22] Y. Xie *et al.*, "Thermally-Reconfigurable Silicon Photonic Devices and Circuits," *IEEE J. Sel. Top. Quantum Electron.*, vol. 26, no. 5, 2020, doi: 10.1109/JSTQE.2020.3002758.

[23] L. Baudzus and P. M. Krummrich, "Efficient low-loss adaptive optical filters based on silicon oxycarbide - Liquid crystal hybrid technology," *Opt. InfoBase Conf. Pap.*, vol. Part F160-, pp.

2019–2021, 2019.

[24] D. Liu, H. Xu, Y. Tan, Y. Shi, and D. Dai, “Silicon photonic filters,” *Microw. Opt. Technol. Lett.*, no. July, 2020, doi: 10.1002/mop.32509.

[25] Y. Gao, X. Sun, P. Li, and D. Zhang, “Polymer Mode Selecting Switch Based on Cascaded MMI Couplers,” *IEEE Photonics Technol. Lett.*, vol. 33, no. 3, pp. 147–150, 2021, doi: 10.1109/LPT.2021.3049414.

[26] M.-Y. Chen and J. Zhou, “Design of add-drop multiplexer based on multi-core optical fibers for mode-division multiplexing,” *Opt. Express*, vol. 22, no. 2, p. 1440, 2014, doi: 10.1364/oe.22.001440.

[27] G. Shi, S. Fu, Q. Sheng, W. Shi, and J. Yao, “Dual-wavelength noise-like pulse generation in passively mode-locked all-fiber laser based on MMI effect,” in *Proc.SPIE*, Feb. 2018, vol. 10512, doi: 10.1117/12.2291225.

[28] M. Khatibi Moghaddam, A. R. Attari, and M. M. Mirsalehi, “Improved photonic crystal directional coupler with short length,” *Photonics Nanostructures - Fundam. Appl.*, vol. 8, no. 1, pp. 47–53, 2010, doi: 10.1016/j.photonics.2010.01.004.

[29] R. Soref, “Tutorial: Integrated-photonic switching structures,” *APL Photonics*, vol. 3, no. 2, 2018, doi: 10.1063/1.5017968.

[30] K. Cooney and F. H. Peters, “Analysis of multimode interferometers,” *Opt. Express*, vol. 24, no. 20, p. 22481, 2016, doi: 10.1364/oe.24.022481.

[31] F. Wang, J. Yang, L. Chen, X. Jiang, and M. Wang, “Optical switch based on multimode interference coupler,” *IEEE Photonics Technol. Lett.*, vol. 18, no. 2, pp. 421–423, 2006, doi: 10.1109/LPT.2005.863201.

[32] “Beam Propagation Methods,” in *Introduction to Optical Waveguide Analysis*, John Wiley & Sons, Ltd, 2001, pp. 165–231.

[33] F. Ahmed Memon, F. Morichetti, and A. Melloni, “Silicon Oxycarbide Waveguides for Photonic Applications,” *J. Phys. Conf. Ser.*, vol. 961, no. 1, 2018, doi: 10.1088/1742-6596/961/1/012014.

[34] A. Arbabi and L. L. Goddard, “Measurements of the refractive indices and thermo-optic coefficients of Si_3N_4 and SiO_x using microring resonances,” *Opt. Lett.*, vol. 38, no. 19, p. 3878, 2013, doi: 10.1364/ol.38.003878.